



Exploring the spatial pattern of community urban green spaces and COVID-19 risk in Wuhan based on a random forest model

Wenpei Li ^a, Fei Dai ^{b,c}, Jessica Ann Diehl ^a, Ming Chen ^{b,c,*}, Jincheng Bai ^d

^a Department of Architecture, College of Design and Engineering, National University of Singapore, 117566, Singapore

^b School of Architecture & Urban Planning, Huazhong University of Science and Technology, Wuhan, 430074, PR China

^c Hubei Engineering and Technology Research Center of Urbanization, Wuhan, 430074, PR China

^d N/A, Allen, TX, 75013, USA

ARTICLE INFO

Keywords:

Urban green spaces
COVID-19
Relative importance
Random forest
Machine learning

ABSTRACT

Since 2019, COVID-19 has triggered a renewed investigation of the urban environment and disease outbreak. While the results have been inconsistent, it has been observed that the quantity of urban green spaces (UGS) is correlated with the risk of COVID-19. However, the spatial pattern has largely been ignored, especially on the community scale. In high-density communities where it is difficult to increase UGS quantity, UGS spatial pattern could be a crucial predictive variable. Thus, this study investigated the relative contribution of quantity and spatial patterns of UGS on COVID-19 risk at the community scale using a random forest (RF) regression model based on (n = 44) communities in Wuhan. Findings suggested that 8 UGS indicators can explain 35% of the risk of COVID-19, and the four spatial pattern metrics that contributed most were core, edge, loop, and branch whereas UGS quantity contributed least. The potential mechanisms between UGS and COVID-19 are discussed, including the influence of UGS on residents' social distance and environmental factors in the community. This study offers a new perspective on optimizing UGS for public health and sustainable city design to combat pandemics and inspire future research on the specific relationship between UGS spatial patterns and pandemics and therefore help establish mechanisms of UGS and pandemics.

1. Introduction

The emergence of coronavirus disease in 2019 (COVID-19) spread rapidly around the world, causing over 14.91 million excess mortalities from January 2020 to December 2021 [1]. Excess mortalities refer to the difference between actual death and the deaths estimated without COVID-19, encompassing both COVID-19 related and indirectly related death [1]. In addition to vaccine, Non-pharmaceutical interventions (NPIs), including protective measures and restrictions, have shown effectiveness against COVID-19 [2,3]. However, the economic losses [4] and the psychological consequences [5] of NPIs have limited their long-term use as preventive measures against pandemics.

Consequently, the urban built environment, which provides settings for human activity, has gained significant attention for its potential role in controlling transmission during a pandemic [6,7]. Among the crucial components of the urban environment, urban green spaces (UGS) play a vital role in promoting public health. UGS, defined as "A wide range of publicly areas that feature natural

* Corresponding author. School of Architecture & Urban Planning, Huazhong University of Science and Technology, Wuhan, 430074, PR China
E-mail address: chen_m@hust.edu.cn (M. Chen).

<https://doi.org/10.1016/j.heliyon.2023.e19773>

Received 21 June 2023; Received in revised form 29 August 2023; Accepted 31 August 2023

Available online 9 September 2023

2405-8440/© 2023 The Authors. Published by Elsevier Ltd. This is an open access article under the CC BY-NC-ND license (<http://creativecommons.org/licenses/by-nc-nd/4.0/>).

vegetation, including grass, plants, or trees. These spaces may include built environmental features, such as urban parks, as well as less managed areas such as woodland and nature reserves [8,9].”, have been demonstrated to be beneficial for public health. The health benefits of UGS includes reducing mortality [10], promoting physical activity [11], alleviating mental stress [12], enhancing mental health and social cohesion [13,14]. Studies also indicated that exposure to and experience in UGS contribute to individuals’ long-term health effects, potentially strengthening individual’s immune system to fight pandemic infection [15,16]. Furthermore, research has revealed a correlation between UGS and pandemics, like the incidence of dysentery tuberculosis and malaria [17] and even COVID-19 [18]. However, most research investigating the relationship with pandemics has primarily focused on assessing the quantity of UGS while overlooking its spatial pattern. Additionally, to our knowledge, no research has explored the relative contribution of various UGS variables to COVID-19, which constitutes the primary focus of this study.

2. Literature review

2.1. The built environment and COVID-19

The built environment encompasses human-made infrastructure and structure, including transportation, UGS, and other public spaces. Several significant pandemics throughout history have promoted modifications in the urban environment to mitigate their transmission [7,19,20]. Examples include the adjusting street patterns following the plague of Athens, developing sewage systems in response to cholera and typhoid fever, and constructing public parks after tuberculosis [7,21,22]. These adjustments in the planning and design of the built environment have been implemented as intervention measures to mitigate the spread of epidemics and have played a crucial role [7,22]. However, with effective medical response and decline in wide-spread pandemics, the concern of urban planner has turned to non-communicable or chronic disease for the past two decades [19]. However, the rapid and severe outbreak of COVID-19 in 2019 renewed the investigation of urban environments and disease transmission. A review of 166 papers indicated that various urban built environment indicators were significantly associated with the risk of COVID-19 [23], including land-use mixture [24–26], commercial land density and facilities [27–29], hospital density [27,30,31], transportation density and accessibility to public transit [24,32], building density, community floor area ratio, absolute fold of community living circle [33–35], and availability of UGS [18,31,36]. Moreover, built environment indicators correlated with COVID-19 transmission varied at different stages of transmission and spatial scopes [29]. More research is needed to explore the relationship between the built environment and COVID-19 risk from different perspectives to inform future urban planning efforts in pandemic control.

2.2. The urban green spaces and COVID-19

The relationships between quantity indicators of UGS and the risk of pandemics has been examined broadly. Quantity indicators of UGS include normalized difference vegetation index (NDVI), UGS area (size), UGS coverage, three-dimensional green space, and so on. For example, NDVI [18,36], country-level annual population-weighted vegetation [37], and county-scale total UGS area and forest [38] in the United States, city-scale NDVI in China [39], UGS coverage (the ratio of UGS area to total area) at the district scale in South Korea [40] and county-scale of the United States [41,42], the ratio of green-blue areas at the county-scale in Poland [43] and street greenness [25] were negatively related to COVID-19 infection. On the other hand, natural area coverage (the ratio of natural area to total area) in India [44], public UGS density in Wuhan, China [30], UGS density in Hong Kong [24], and higher Visible Green Index calculated from street view image [45] showed a positive correlation with COVID-19 cases. The inconsistent relationships between quantity indicators and COVID-19 infections varied may be attributed to factors such as the research scale, geographic location, and the stage of the COVID-19.

The spatial pattern of UGS may be another reason for the inconsistent relationships between UGS and COVID-19. The spatial pattern of UGS refers to the internal arrangement and spatial characteristics of UGS, such as shape, aggregation, fragmentation, connectivity, and dispersions. Understanding these spatial pattern metrics enable us to understand their influences on the surrounding environment, such as temperature, humidity, and particulate matter. These factors, in turn, can affect the survival time of COVID-19 virus and transmission risk within the built environment [46,47]. Studies have shown that connected and aggregated green spaces exhibit a stronger relationship with temperature and PM_{2.5} reduction [48,49]. Some studies indicate when UGS is small and continuous rather than fragmented, park usage is associated with reduced residual case rates [50]. On the other hand, highly connected public UGS has been shown to correlate with high risk of infection transmission [51]. Although the results are inconsistent, these studies underscore the importance of considering UGS spatial pattern in relation to COVID-19 risk. Moreover, given the challenges of increasing the quantity of UGS in densely populated cities, optimizing UGS from perspective of spatial pattern can provide a feasible alternative solution. However, studies exploring the associations between UGS spatial patterns and COVID-19 risk remain limited.

Currently, spatial pattern indexes used to examine influence on COVID-19 are typically calculated using Fragstats software, which is called landscape pattern metrics. For instance, metrics like connectivity (CONTAG) and the dispersion of UGS (Interspersion and Juxtaposition index) have shown high explanatory power for the number of COVID-19 cases and the rate of increase of COVID-19 cases [52]. However, Fragstats can only provide quantitative values of UGS spatial pattern and cannot visualize the spatial location of UGS. Therefore, even with results of specific influence of UGS spatial patterns on COVID-19, proposing an effective approach optimizing UGS morphology and mitigate the risk of pandemic is challenging. Morphological spatial pattern analysis (MSPA), an image-processing method that uses mathematical morphology concepts, can improve the prior standard landscape-configuration-metrics-based pattern analysis based on Fragstats [53,54].

MSPA can identify the characteristics of hubs, corridors, and boundaries through a series of mathematical morphology operators

and image-processing techniques. This analysis enables the assessment and optimization of UGS by categorizing them into seven mutually exclusive classes, providing a visual representation of their spatial distribution attributes and corresponding physical environmental implications at the pixel level [54]. MSPA has garnered attentions across different spatial scales and objectives, including its associations with urban heat, atmospheric PM levels and air pollution concentration [49,55,56]. Moreover, MSPA has been effectively utilized in assessing land use and environmental conditions. For example, Lin et al. [57] created an assessment framework based on MSPA to improve protected areas. Wickham et al. [58], conducted a national assessment of green infrastructure and its changes in the United States. These findings provide valuable insights for mitigating urban heat and PM_{2.5} pollution, as well as facilitating land use planning and UGS management, particularly in situations where increasing UGS quantity is constrained.

2.3. Methods to explore the potential factors of COVID-19

Typically, existing studies adopt Pearson or Spearman correlation models to probe the link between COVID-19 risk and variables related to demographic, socioeconomic factors, and the built environment. Additionally, geographically weighted regression models [59], negative bivariate generalized linear mixed models [40], ridge regression models [37], and ANOVA-based geographic detector models [60] have been applied to examine the association between potential variables and COVID-19 risk. However, these traditional methods require data to follow certain rules, such as a normal distribution and no collinearity between independent variables. In some cases, fine-grained disease data cannot meet these requirements. In this vein, machine learning, like random forest (RF) models, may provide a solution. RF models can handle complex nonlinear relationships and intercorrelations between input variables. Further, existing studies showed that RF regression models improved the accuracy of model prediction compared to traditional methods and can be used for classification and regression [61]. Importantly, RF models can measure variables' importance through permutation [62]. RF regression models have been employed to examine the relative contribution of various built environmental indicators on land surface temperature [63], PM_{2.5} variations [61], and carbon emissions [64]. Therefore, an RF model can be adopted to investigate the significance of different UGS indicators and compare the contribution of UGS spatial pattern and quantity.

Most existing research has concentrated on exploring the correlation between the COVID-19 and UGS quantity metrics. UGS spatial pattern metrics have largely been ignored. In addition, UGS needs to be optimized from a new perspective in post-pandemic era, considering that there is little space for increasing UGS quantity in most of nowadays high-density communities. As for research unit, existing studies investigating the effects of UGS on COVID-19 are mainly based on region, city, and county scale, with limited attention at the community scale. However, the community is the place where residents are most exposed daily, and the physical environment of the community may affect residents' behavior and the spread of pandemics. Further, impacts of UGS on COVID-19 risk in different areas at larger, aggregated scales are complex and even opposite which could be attributed to ecological fallacy, thus more studies at the granular community scale are needed to enrich the research on the mechanism of UGS effects on pandemics.

Given the aforementioned gaps, this study aims to probe the relative importance of the UGS quantity and spatial pattern metrics of community-scale UGS on the risk of COVID-19 by applying a RF regression model. We hypothesize that UGS coverage at the community scale based on a RF model is a stronger predictor than some of the MSPA classes. Based on findings from this research, the possible mechanisms between UGS and the risk of causing COVID-19 will be discussed. As far as we know, MSPA is adopted for the first time to examine the influence of UGS spatial pattern on public health. This study can provide additional evidence regarding the health benefits of UGS, new potential metrics to explore the relationship between UGS and pandemics and new UGS optimizing perspective for healthy city planning guidelines to cope pandemic. This paper is organized as follows. Section 1. "Introduction" provides the background of COVID-19 and its relationship with UGS. Section 2. "Literature review" synthesized existing studies. Section 3. Introduces the methodology used to build the models, including the research site, sample selection, data collection and calculation of variables, and model setting. Section 4. Describes the results of variable calculation and RF model. Section 5. and 6. Present the discussions and conclusions.

3. Methodology

3.1. Research site overview

Prior to March 2020, Wuhan suffered the most severe impact of COVID-19 in comparison to other cities worldwide. Its mega-city attributes and well-developed transportation accelerated the spread of this disease. Wuhan is located on the plain in the middle and lower reaches of Yangtze River, situated in the eastern region of Hubei Province, China. It comprises the main urban area and new town, with the main urban area consisting of three towns, namely Hankou (Jiangnan district, Jiangan district, and Qiaokou district), Hanyang (Hanyang district), and Wuchang (Wuchang district, Hongshan district and Qingshan district), covering a total of seven administrative districts. According to the seventh National Population Census of Wuhan, as of November 1, 2020, the city's permanent population is 12,326,518. By December 1, 2020, the overall count of confirmed COVID-19 cases in Hankou comprised 49% of the affected population in central urban area and 37% of the total affected population in the city. One initial epicenters of COVID-19 in Wuhan, Huanan Seafood Market, is centrally located in Hankou with a complex and diverse range of surrounding buildings and land use types. This research specifically focused on the community scale in Hankou.

3.2. Sample community selection

The presence of rivers and water systems can influence the flow of energy and materials, resulting in variation in population density

and economic development among the three towns of Wuhan, which are separated by the Yangtze and Han River. For this study, the focus is Hankou, where the initial epicenter of COVID-19 (Huanan Seafood Market) is located. Infectious disease outbreaks generally exhibit significant morphological and temporal aggregation. Since COVID-19 has not been found to spread by banding factors such as rivers, a buffer zone was used to delimit the research area. Specifically, this study targeted communities located within a 3.5 km radius buffer zone centered on the Huanan Seafood Market, since the buffer zone exceeding 3.5 km in radius would have extended beyond the administrative district of Hankou. Moreover, considering that COVID-19 is characterized by aggregated outbreaks, with more than one confirmed case or asymptomatic infected individual identified within a small area over 14 days [65], interpersonal transmission through close contact likely plays a significant role in the spread of the pandemic. Accordingly, communities with less than two cases of COVID-19 were excluded. Furthermore, through on-site investigation, communities that belong to staff dormitories, as well as those with blurred boundaries and limited UGS that were unsuitable for MSPA analysis were excluded from the study. Ultimately, a total of 44 sample communities in this study were obtained (Fig. 1).

3.3. Prevalence rate of COVID-19

Prevalence rate, which is the number of cases per 100,000 people, has commonly been adopted as an indicator of COVID-19 risk in previous studies at various scales, such as administrative, urban, and national scales [38,40,66]. Other studies have utilized different indicators to assess COVID-19 prevalence risk, including the number of cases [31,41,50], the ratio of confirmed cases and total population in research unit [36], and the degree of population aggregation [33]. As the community population is usually smaller than 100,000, it is improper to use the widely adopted prevalence rate of COVID-19. Additionally, the number of COVID-19 cases tends to ignore the impact of the total community population on pandemic risk. Therefore, the ratio of confirmed cases and total population in a research unit is a better proxy for COVID-19 risk. However, fine-grained total population in the community are generally not available and total number household in community that can be an alternative. Thus, for this study, the risk of COVID-19 was defined as the ratio of COVID-19 cases to the total number of households within the community.

The data for calculating COVID-19 prevalence rate were extracted from the Community Infection Count Checker website (<http://2019ncov.com/>) provided by China [33]. The data for this website is sourced from local health commissions and also accepts voluntary feedback. The website was launched on February 7, 2020, and discontinued 17 days later on February 24. The number of households in the sampled communities was extracted from the China Community Network and Lianjiang Real Estate (<https://wh.lianjiang.com/>).

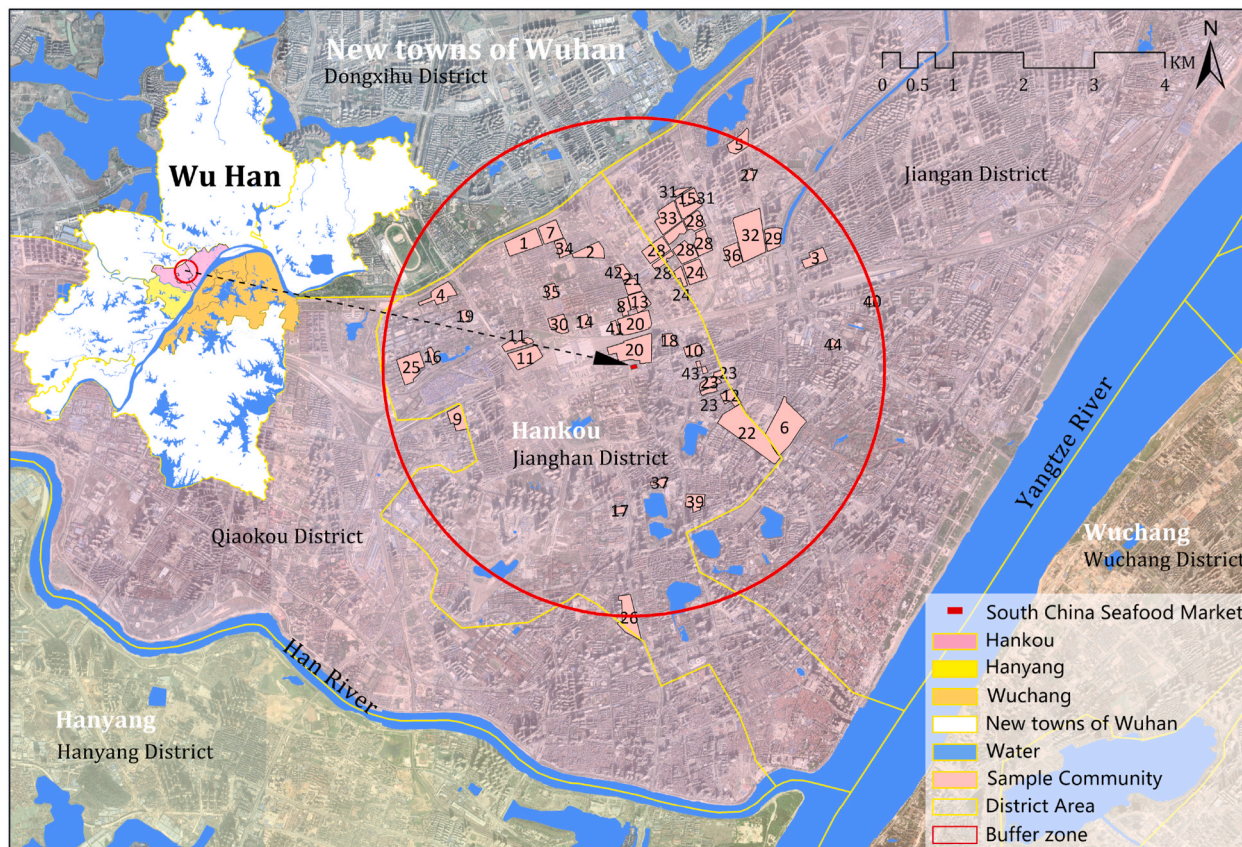


Fig. 1. Location of research site and sample communities.

Both of these data sources have been previously utilized in previous academic research [33,67,68].

3.4. Green spaces variables and calculation

In this study, we adopted green spaces coverage to assess the quantity of UGS. Specifically, green spaces coverage is the ratio of extracted green space area to the total area of the community. Indicators of spatial patterns of UGS in this study were calculated using MSPA.

The scope of each community was obtained from Baidu Maps, and on-site field investigation was conducted to ensure community boundaries and extract UGS. High-resolution remote sensing images (0.26 m) from Google Earth were downloaded on December 26, 2019, and processed using ArcGIS 10.2 to map UGS. The area of UGS in each community was then obtained. Before performing MSPA, the extracted UGS was reclassified as foreground (assigned a value of 2) and other lands as background (assigned a value of 1). The binary raster image data in TIFF format was obtained and imported into GuidosToolbox software to conduct MSPA (Fig. 2). Through image processing procedures, UGS in the research unit was classified into seven non-overlapped morphological classes. The seven MSPA classes were UGS patches of varying shapes and sizes (Table 1 and Fig. 3 a, b). The structural elements and edge width were two main parameters affecting the MSPA results. As for structural elements, adopting eight neighborhoods (four neighborhoods) means that the foreground pixel calculated was merged with the surrounding eight (four) pixels. Similar to other research [48,69], eight neighborhood were adopted for structural elements. The edge width determined the condition of how well the MSPA results reflected the UGS actual condition. Specifically, as the edge width increased, the minimum core size increased, and the number of core patches decreased, which could convert a small core UGS class to an islet. To maximize the actual picture of UGS in all communities with different sizes, an edge width value of 11 was adopted to gain more detailed information on the UGS spatial pattern. With Equation (1), the proportion of each MSPA class in each community was calculated as the UGS spatial metrics.

$$MSPA_i = S_i / S \quad (i = 1, 2, \dots, 7) \tag{1}$$

Where $MSPA_i$ refers to the proportion of each MSPA class including core, islet, ...perforation (%); S_i refers to the area of each MSPA class (m^2); and S means the area of each community (m^2).

3.5. Variable importance via random forest

The intricate relationship between COVID-19 prevalence and various UGS variables, along with the intercorrelation between seven MSPA classes, rendered traditional statistical models unsuitable. However, RF models have been shown good performance in small sample size analysis when compared with other machine learning models and traditional regression models [70]. Therefore, given the small sample size of 44 communities, this study adopted an RF model to investigate the relative importance of varied UGS indicators on the COVID-19 prevalence. Specifically, UGS coverage and 7 MSPA classes were regarded as explanatory variables respectively and the prevalence rate of COVID-19 served as the dependent variable.

The RF model, proposed by Leo Breiman [62], is an integrated algorithm based on a decision tree. It employs bootstrap resampling to randomly and repeatedly select n samples from the initial training set, establishing n decision trees. This process introduces randomness to the split samples and variables, enhancing the independence between trees and reducing the likelihood of model overfitting. As for RF model building, the number of decision trees ($ntree$) and the number of variables used per tree ($mtry$) are two essential hyperparameters. Using the optimal hyperparameters that significantly affect the performance of the model can maximize the accuracy of the model [71]. The model's root mean squared error (RMSE), representing the average difference between the observed dependent variables and predicted values, was used as the metric to evaluate the model's performance. The lower RMSE, the higher accuracy of the model. To determine the best $ntree$ and $mtry$, cross-validation was performed to assess the accuracy of the RF model by testing different combinations of these hyperparameters. Take the 10-fold cross-validation as an example, the input data can be partitioned into ten subsets, and the RF model calculates the RMSE when each subset is used as the testing data. The final RMSE is obtained by averaging the ten RMSE values from each calculation. Subsequently, the $ntree$ and $mtry$ values of the model with the

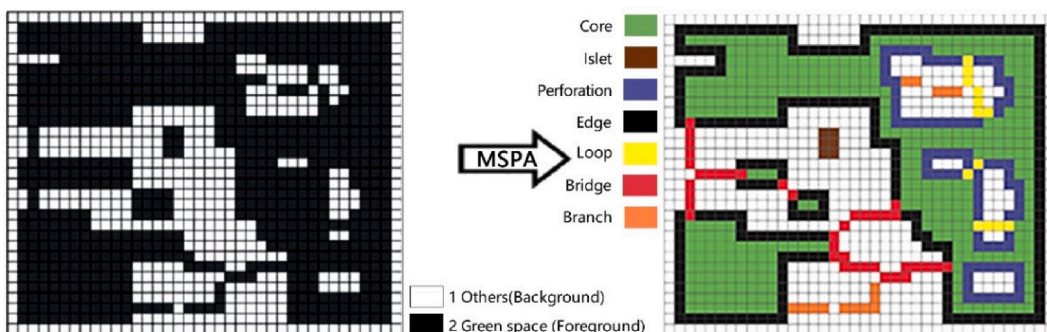


Fig. 2. Example of seven morphological patterns (Data source [54]).

Table 1
Ecological definition of seven morphological patterns.

MSPA classes	Definition
Core	Large green patches, like community center parks, large group green space
Islet	Small, fragmented, relatively low-connected green patches, like pocket parks, rooftop gardens, and green spaces next to houses
Perforation	The internal boundary of the core area with edge effect, like impervious area for entertainment in large green spaces in communities
Edge	External boundary of the core area with edge effects, which can protect the ecological stability within the core, like the green belt at the edge of the community center park
Loop	Internal corridors within the core create shortcuts for species migration and strengthen the energy flow in the core, like the edge of the impervious area in the green space
Bridge	Connected to the core area, which is a corridor for material and energy exchange between patches, like the green belt of roads and ribbon green space within the community
Branch	Remnant areas of green space that are linked to the core on only one side, like the green belt of the road

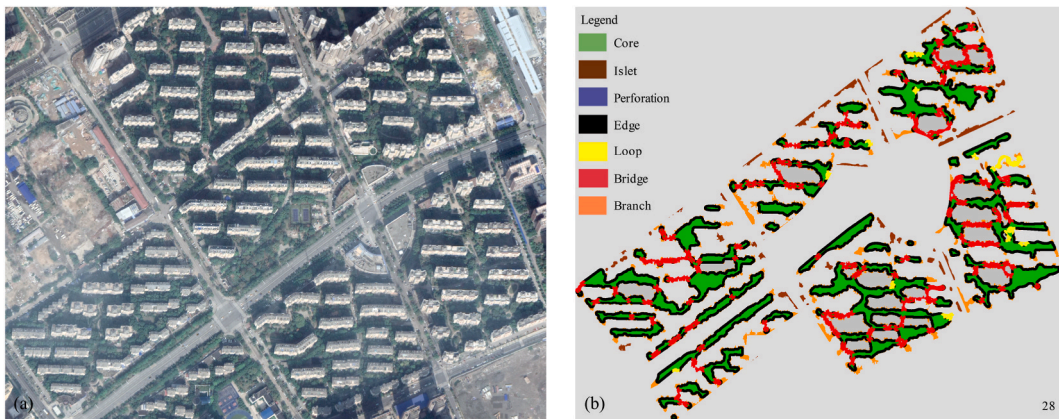


Fig. 3. Example of initial Google image (a) and MSPA result (b) of sample community 28.

lowest final RMSE are selected to build the final RF model and determine the relative importance of the various factors. Based on cross-validation, methods such as Grid search, Bayesian optimization, various packages in R studio, and professional experience can help obtain the best hyperparameters [71,72].

In this research, the “ParamHelpers” package was adopted to adjust a hyperparameter and a 10-fold cross-validation was performed to validate the selected hyperparameter. The performance of model was evaluated using “% var explained”, which is similar to the coefficient of determination R^2 of traditional regression mode. The best model, with the lowest RMSE and highest “% var explained” was selected. The relative influence of the independent variables was measured by the reduction in mean square residuals based on random permutations (%IncMSE) or the reduction in model precision (Inc Nodularity). This research used %IncMSE to measure the importance of the independent variables since it is the most widely adopted metric, with a higher %IncMSE indicating a more predictive variable.

The RF analysis was conducted in R 4.1.2 using the “RandomForest” package for model building. To assess the significance of each

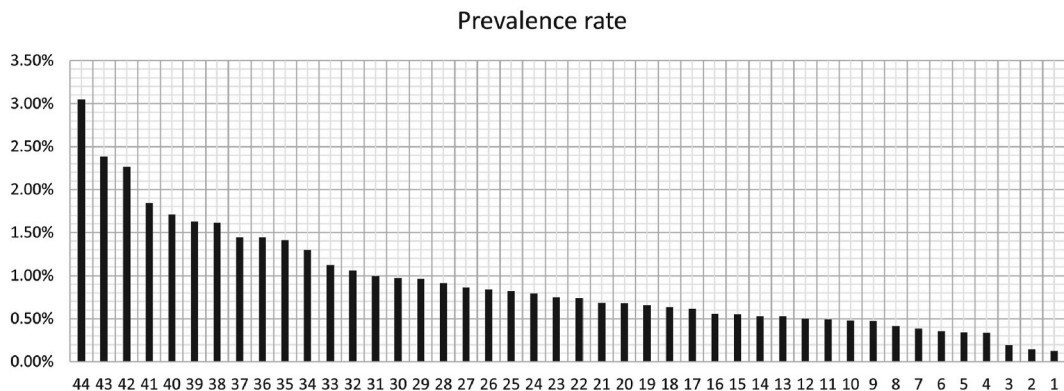


Fig. 4. The prevalence rate of COVID-19 among sample communities.

independent variable on the dependent variable, the “permute” package was adopted. The “A3” package was used for assessing the significance of the full model and cross-validate the R^2 values [73].

4. Results

4.1. Prevalence rate of COVID-19

Among the 44 sample communities, the prevalence rate of COVID-19 varied, with the highest being 3.048% and the lowest being 0.126% (Fig. 4). Out of these communities, 31 sample communities reported prevalence rates ranging from 0.126% to 1.060%, with 20 of them having prevalence rates between 0.504% and 1.060%. The remaining 13 communities had prevalence rates between 1.060% and 3.048%.

4.2. Green spaces coverage in sample communities

Overall, the green spaces coverage in the sample communities ranged from 15.542% to 51.382%, and these values could be divided into five tiers (Fig. 5). Notably, the two communities with less than 20% green spaces were older communities built before 2000. Most of the sample communities were covered by greenery between 20% and 50%, among which the number of communities with greenery coverage of 20%–30%, 30%–40%, and 40%–50% were 12, 18, and 10, respectively. Only two communities had a green spaces coverage rate greater than 50%.

4.3. Spatial patterns of green spaces in sample communities

According to the average percentage of MSPA classes (Fig. 6), the predominant type of communities in the samples were edge-dominated, where the edge class served as the primary constituent, accounting for an average of 32.21%. This dominance can be attributed to the unique characteristics of the research unit in this study, which focused on a community with an unconventional green spaces in the form of an octopus-shaped road green belt. Consequently, this kind of complex shape of the core patch in the community resulted in a higher proportion of edge. The average percentage of core and islet classes represented the second-tier components, with their average ratios being roughly half that of the edge, at 18.72% and 17%, respectively. The proportion of linear elements, including branches and bridges, accounted for 14.72% and 14.83% respectively. In contrast, the presence of loop and perforation elements was relatively lower compared to the other classes, with the majority of communities showing 0% occurrence of these two indicators. On average, the proportions of loop and perforation were only 2.47% and 0.06%, respectively.

4.4. Random forest results and analysis

The optimal hyperparameters from the “ParamHelpers” package were 736 for ntree, 2 for mtry. The R^2 value of the RF regression model was 35.4%, implying that more than 35.4% of COVID-19 prevalence can be explained by the 8 selected UGS indicators. The relative importance of the 8 factors to COVID-19 prevalence is shown in Fig. 7. The order of four important variables was edge, core, loop, and branch. The relative importance of eight UGS metrics generated from the RF model reveals that MSPA indices of community green spaces shows greater influence than coverage in this study. Specifically, the influence of edge and core is in the first rank and the difference between the two is small. It may be because that the core is the relatively large and mainly functional green spaces at the community scale, and thus is the main indicator for influencing various environmental factors and residents’ activities. In addition, the edge is peripheral green spaces to the core and thus are influenced to some extent by the core share, since the more complex the core shape the more the edge share. While green spaces on a community scale is limited in size and thus may render the effects of these two indicators comparable. The effects of loop and branch also showed significance and the difference between the two are also small. The

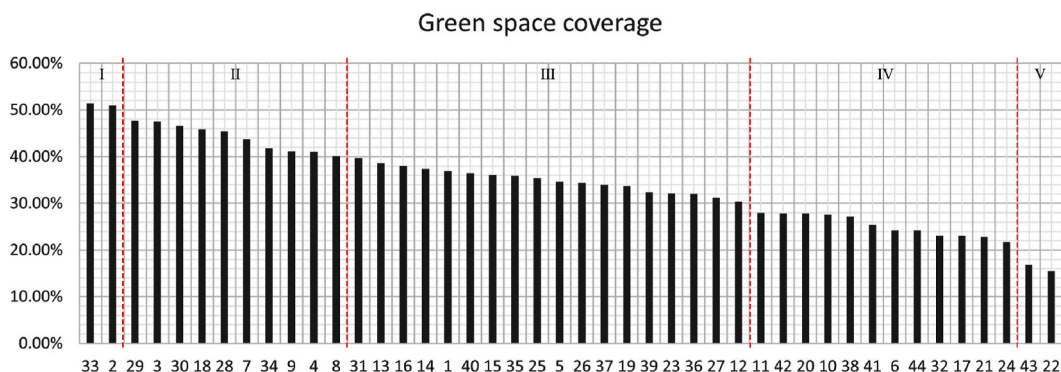


Fig. 5. Green space coverage of sample communities.

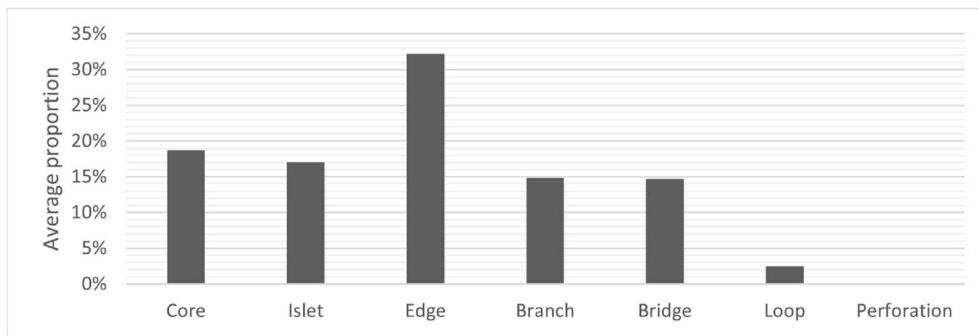


Fig. 6. The average percentage of each MSPA class in sample communities.

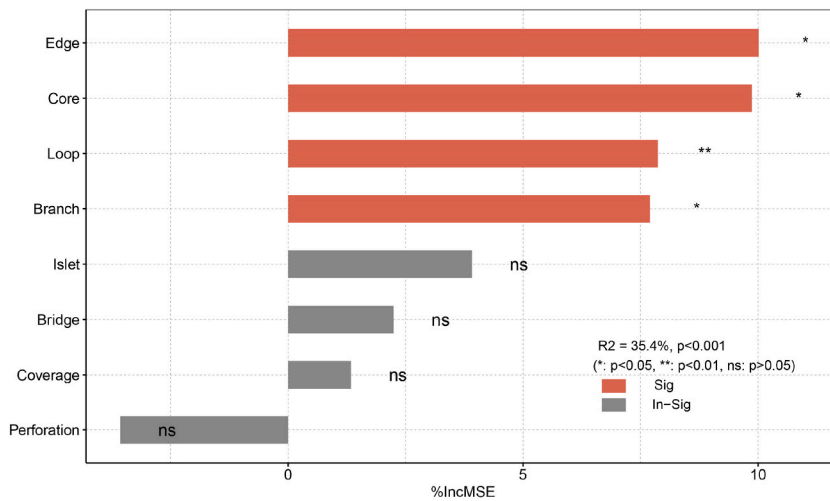


Fig. 7. Importance ranking of factors.

rest of the indicators showed a small and insignificant impact.

5. Discussion

In this research, we attempt to emphasize the importance of UGS spatial pattern on COVID-19 prevalence, as the majority of existing studies primarily focus on UGS quantity. To do this, the relative importance of UGS spatial pattern metrics and UGS quantity on community scale was examined using RF model. Findings indicated that the UGS spatial pattern at the community level holds better predictive power for COVID-19 risk compared to UGS quantity. In addition to controlling residents' social distance, which is affected by residents' clustering and dispersal behaviors and represents a core pathway of NPIs, increasing evidence highlights the impact of environmental factors on COVID-19 transmission [74,47]. In light of these two pathways, this study considered possible mechanisms by connecting the key findings to other relevant literatures that explores the influence of UGS on environmental factors and residents' social distance.

5.1. Potential mechanisms between urban green spaces and COVID-19

Findings from this study highlight the importance of UGS spatial pattern in relation to COVID-19 risk by presenting the relatively lower importance of UGS quantity at the community scale. The RF model used in this study provides only relative importance of the factors, and therefore the specific influence of UGS on the risk of COVID-19 cannot be determined. More broadly, existing results of the relationship between UGS coverage and risk of COVID-19 have also not been uniform because of varied locations, metrics, and methods. For instance, research in the United States has shown that a 1% increase in the percentage of urban vegetation would result in a 2.6% decrease in cumulative COVID-19 cases, and the role of population density and baseline infection may be attenuated by the mediating effect of urban vegetation [41]. And the per capita parkland area in the Pearl River Delta showed a high explanation rate for the growth rate of COVID-19 infection [52]. Conversely, UGS in other locations, such as India [44] and Hong Kong [24] showed a positive correlation with the risk of COVID-19. Additionally, a study on open space presented a mixed association with COVID-19

infection, with forest use outside a park benefiting people more than forest use inside a park [38]. Moreover, at the community level, the proximity of UGS displayed both strong positive and negative correlation with COVID-19 risk in different communities in Wuhan [33]. The discordant results across different studies points to a need to explore metrics other than total quantity of UGS.

Existing mixed results may also be due to the influence of UGS on several environmental factors that indirectly influence the prevalence of COVID-19. On the one hand, COVID-19 has been shown to be aerosol-transmissible and environmental factors may influence the incidence by affecting the survival time of virus in the air [75,76]. For instance, the prevalence of COVID-19 has been demonstrated to be related to air quality, air pollutants, temperature, and humidity [77–81]. Furthermore, particulate matter identified as a carrier for the virus can increase the long-distance viral diffusion and further affect COVID-19 risk in communities [82]. A comprehensive study in Wuhan and Xiaogan suggested that AQI and all pollutants were positively associated with daily COVID-19 prevalence, while the air temperature was negatively associated with COVID-19 prevalence [83]. On the other hand, an increase in UGS coverage at the neighborhood scale can increase humidity [84], decrease the air temperature [85], and reduce fine air particle [86]. Lower temperature is conducive to virus survival, which may lead to an increase in prevalence; while increased humidity and the lower concentration of aerosols and particulate matter deposited in the air has been shown to decrease COVID-19 cases [87]. Thus, both conducive (lower temperature) and detrimental (higher humidity, lower particulate matter and better air quality) environmental factors for virus transmission lead by more UGS may account for current inconsistent results between environmental factors and the risks of COVID-19.

As for the effect of UGS quantity on social distance among residents, large UGS, corresponding to the core patches of the community UGS, provide more public space for residents and therefore are easier to increase the risk of disease transmitting since the increased possibility of residents encountering each other [51]. This may appear contradictory to the prevailing evidence indicating a negative correlation between UGS quantity indicators and COVID-19 infection indicators. This apparent contradiction might imply the presence of a threshold for UGS quantity and core patch size in community, where both excessively high and low levels could contribute to an elevated risk of transmission. Exploring this threshold could be a valuable avenue for future research.

Spatial patterns of UGS, as captured by the MSPA classes, may affect the prevalence of COVID-19 through environmental factors and social distance within communities. For example, MSPA classes have shown significant correlations with environmental factors, like atmospheric particulate matter and temperature. Thus, MSPA classes may affect the survival time of COVID-19 virus, as well as affect aerosol-based transmission by influencing environmental indicators, like temperature and humidity. Relatedly, the RF model in this study suggests that the core, edge, branch, and loop patterns were the most significant and influential among the eight variables. These four classes were also effective variables in previous studies which probed the relationship between MSPA classes and environmental factors. For example, core, edge, and branch ratio were more effective in optimizing PM2.5 levels at varying pollution concentrations at the neighborhood scale [48]. In addition, core, edge, and loop ratio have been found to be more associated with the mean temperature and temperature range of the neighborhood than other MSPA classes [49]. Finally, the correlation between MSPA classes and the mean temperature was found to be more significant when the core accounted for more of the neighborhood UGS.

MSPA classes may also affect COVID-19 prevalence by affecting residents' social distance and the degree of aggregation of residents within communities. MSPA classes can manifest the connectivity of UGS, like more islet patterns mean higher fragmentation and more bridge patterns mean higher aggregation. A study in UK showed that the use of small and continuous UGS was associated with a decrease in pre-existing cases, although the mobility of people remained the key measure [50]. However, in another study, highly connected UGS with high choice measures showed a correlation with high risk of infection transmission [51]. Therefore, a UGS with proper MSPA classes ratio may assist in regulating people's social distance while providing outdoor activities, which in turn may reduce the transmission risk of COVID-19. In an era demanding to mitigate pandemic transmission requires the control of population movement and social distance of people, and morphological pattern of UGS needs to be further explored.

5.2. Significance and implications

To the best of our knowledge, the relative contribution of UGS spatial pattern and UGS quantity on COVID-19 prevalence was examined for the first time. This research extends our knowledge and understanding concerning the role of spatial pattern of UGS in the relationship between UGS and pandemics. Although some previous studies have explored the effects of UGS spatial patterns on COVID-19 risk, UGS spatial patterns remain under study. This research found that spatial patterns of UGS at the community scale are more important variables affecting the prevalence of COVID-19 compared to UGS quantity. Compared to research emphasizing more quantity of UGS contributed to less COVID-19 risk, which is difficult to increase in built-up communities and high-density cities, optimizing UGS spatial pattern could be more feasible. Second, these findings and mechanisms discussed above suggest that MSPA metrics could be an important potential variable related to the risk of pandemics, mediating the relationship between UGS quantity and the risk of COVID-19. The MSPA method used to measure the morphological patterns of UGS in this research can help in visualizing UGS patterns and therefore provide new ways of optimizing community UGS to mitigate COVID-19 risk. Finally, this research also enriches the knowledge and understanding of existing literature on the impact and mechanisms of the quantity and spatial patterns of UGS on pandemics.

5.3. Limitations and future opportunities

However, this research is subject to certain limitations. Firstly, the availability of fine-grained data is limited, such as the proportion of cases infected by family members and cases infected by other residents in the community. Additionally, due to the lack of precise population information for the communities, the risk of COVID-19, namely the prevalence rate, was calculated utilizing household

data instead of the precise population of the communities. Consequently, there is a possibility of overestimating the risk of COVID-19 within each community. These may affect the results of quantitative analysis and restrict the generalizability of the findings to a specific study area and timeframe, representing characteristics only during the initial transmission stage. Second, since the focus of this research was UGS, only indicators of UGS were included in the RF model and the explanatory power for the overall model was relatively low. Third, the relative importance via RF model does not generate a causal relationship between UGS factors and risk of COVID-19. However, the RF model is still useful as an initial phase of key variable selection. Finally, no control variables were included. Although sample communities were carefully selected to control the social-economy factors as much as possible, models that include other factors such as population density, transportation routes and modes, lifestyle, income, and occupation, as well as environmental elements of the neighborhood (e.g., building density, floor area ratio, building height, temperature, and humidity) may be able to better reveal the mechanisms between UGS and COVID-19 prevalence. Considering the limited academic attention on this topic thus far, it is imperative to conduct replication studies and further explore the potential mechanisms. Future investigations should delve into the detailed relationship between UGS spatial patterns and pandemics risk. Exploring whether the UGS spatial patterns mediated the results from UGS quantity metrics and the risk of pandemics will also be important.

6. Conclusion

In this research, the RF model was adopted to investigate the relative significance of UGS quantity and UGS spatial pattern metrics in relation to the prevalence of COVID-19 at the community scale. Among the various UGS variables, four MSPA variables were identified as the most important factors, ranked in the following order: core, edge, branch, and loop. In addition, according to the findings from the RF model, the potential mechanisms through which UGS may influence the prevalence rate of COVID-19. These mechanisms encompassed its possible influence on resident's clustering and dispersal behaviors as well as its probable impact on environmental factors such as temperature, humidity, particulate matter, and air quality, all of which may affect the survival time of COVID-19 virus and disrupt the transmission process. The study's findings hold implications for urban planners as they underscore the potential impact of spatial pattern of UGS on public health. This reinforces the importance of considering these indicators into account when examining the role of environmental contributors to public health outcomes. Despite some limitations, the results offer a novel perspective on optimizing UGS for public health and pandemic-resistant city design. They inspire further research into the relationship between UGS spatial patterns and pandemics, thereby aiding the understanding of UGS-pandemic mechanisms. Lastly, the study also underscores the importance of exploring new metrics for assessing the relationship between UGS and pandemic risks.

Author contribution statement

Wenpei Li: Conceived and designed the experiments; Performed the experiments; Analyzed and interpreted the data; Contributed reagents, materials, analysis tools or data; Wrote the paper.

Fei Dai; Jessica Ann Diehl; Jincheng Bai: Contributed reagents, materials, analysis tools or data.

Ming Chen: Conceived and designed the experiments; Contributed reagents, materials, analysis tools or data.

Data availability statement

Data will be made available on request.

Declaration of interest's statement

The authors declare no conflict of interest.

Declaration of competing interest

The authors declare that they have no known competing financial interests or personal relationships that could have appeared to influence the work reported in this paper.

References

- [1] Global Excess Deaths Associated with COVID-19, January 2020 - December 2021, World Health Organization, 2022. <https://www.who.int/data/stories/global-excess-deaths-associated-with-covid-19-january-2020-december-2021>.
- [2] K. Prem, et al., The effect of control strategies to reduce social mixing on outcomes of the COVID-19 epidemic in Wuhan, China: a modelling study, *Lancet Public Health* 5 (5) (2020) e261–e270, [https://doi.org/10.1016/S2468-2667\(20\)30073-6](https://doi.org/10.1016/S2468-2667(20)30073-6).
- [3] D. Rojas-rueda, Built Environment, Transport, and COVID-19: Review 8 (2021) 138–145, <https://doi.org/10.1007/s40572-021-00307-7>.
- [4] M. Škare, D.R. Soriano, M. Porada-Rochoń, Impact of COVID-19 on the travel and tourism industry, *Technol. Forecast. Soc. Change* 163 (April 2020) 2021, <https://doi.org/10.1016/j.techfore.2020.120469>.
- [5] M. Personal, R. Archive, K. Le, M. Nguyen, The psychological consequences of COVID-19 lockdowns, *Int. Rev. Appl. Econ.* 35 (2) (2021) 147–163, <https://doi.org/10.1080/02692171.2020.1853077>.
- [6] A.J. Scott, M. Storper, Current Debates in Urban Theory: a Critical Assessment," *Urban Stud.* 53 (6) (2016) 1–36.
- [7] H.A.A. Hussein, Investigating the role of the urban environment in controlling pandemics transmission: lessons from history, *Ain Shams Eng. J.* 13 (6) (2022), 101785, <https://doi.org/10.1016/j.asej.2022.101785>.

- [8] L. Taylor, D.F. Hochuli, Defining greenspace: multiple uses across multiple disciplines, *Landsc. Urban Plann.* 158 (2017) 25–38, <https://doi.org/10.1016/j.landurbplan.2016.09.024>.
- [9] K. Lachowycz, A.P. Jones, Towards A better understanding of the relationship between greenspace and health: development of A theoretical framework, *Landsc. Urban Plann.* 118 (2013) 62–69, <https://doi.org/10.1016/j.landurbplan.2012.10.012>.
- [10] M.I. Kasdagli, K. Katsouyanni, K. de Hoogh, P. Lagiou, E. Samoli, Associations of air pollution and greenness with mortality in Greece: an ecological study, *Environ. Res.* 196 (2021), 110348, <https://doi.org/10.1016/j.envres.2020.110348>.
- [11] J. Maas, R.A. Verheij, P. Spreeuwenberg, P.P. Groenewegen, Physical activity as a possible mechanism behind the relationship between green space and health: a multilevel analysis, *BMC Publ. Health* 8 (2008) 1–13, <https://doi.org/10.1186/1471-2458-8-206>.
- [12] K.M.M. Beyer, A. Kaltenbach, A. Szabo, S. Bogar, F. Javier Nieto, K.M. Malecki, Exposure to neighborhood green space and mental health: evidence from the survey of the health of Wisconsin, *Int. J. Environ. Res. Publ. Health* 11 (3) (2014) 3453–3472, <https://doi.org/10.3390/ijerph110303453>.
- [13] V. Jennings, O. Bamkole, The relationship between social cohesion and urban green space : an avenue for health promotion, *Int. J. Environ. Res. Publ. Health* 16 (3) (2019) 452, <https://doi.org/10.3390/ijerph16030452>.
- [14] P. Dadvand, X. Bartoll, X. Basagaña, A. Dalmau-bueno, Green spaces and general health : roles of mental health status, Social Support , and Physical Activity 91 (2016) 161–167, <https://doi.org/10.1016/j.envint.2016.02.029>.
- [15] S.J. Slater, R.W. Christiana, J. Gustat, Recommendations for keeping parks and green space accessible for mental and physical health during COVID-19 and other pandemics, *Prev. Chronic Dis.* 17 (17) (2020) 1–5, <https://doi.org/10.5888/PCD17.200204>.
- [16] C. Twohig-Bennett, A. Jones, The health benefits of the great outdoors: a systematic review and meta-analysis of greenspace exposure and health outcomes, *Environ. Res.* 166 (2018) 628–637, <https://doi.org/10.1016/j.envres.2018.06.030>.
- [17] L. Liu, Y. Zhong, S. Ao, H. Wu, Exploring the relevance of green space and epidemic diseases based on panel data in China from 2007 to 2016, *Int. J. Environ. Res. Publ. Health* 16 (14) (2019), <https://doi.org/10.3390/ijerph16142551>.
- [18] E.N. Spotswood, et al., Nature inequity and higher COVID-19 case rates in less-green neighbourhoods in the United States, *Nat. Sustain.* 4 (12) (2021) 1092–1098, <https://doi.org/10.1038/s41893-021-00781-9>.
- [19] W.B. Freilich, The built environment and its relationship to the public's health: the legal framework, *Am. J. Publ. Health* 93 (9) (2003) 1390–1394, <https://doi.org/10.1177/009286158602000405>.
- [20] J. Davis, Epidemics, planning and the city: a special issue of planning perspectives, *Plann. Perspect.* 37 (1) (2022) 1–8, <https://doi.org/10.1080/02665433.2022.2019982>.
- [21] R.A. Plunz, et al., Twitter sentiment in New York City parks as measure of well-being, *Landsc. Urban Plann.* 189 (May) (2019) 235–246, <https://doi.org/10.1016/j.landurbplan.2019.04.024>.
- [22] R. Reyes, R. Ahn, K. Thurber, T.F. Burke, Urbanization and infectious diseases: general principles, historical perspectives, and contemporary challenges, in: *Challenges in Infectious Diseases*, Springer, 2013, pp. 1–319.
- [23] M. Alidadi, A. Shari, Effects of the built environment and human factors on the spread of COVID-19: a systematic literature review, *Sci. Total Environ.* (2022), 158056, <https://doi.org/10.1016/j.scitotenv.2022.158056>.
- [24] J. Huang, M.P. Kwan, Z. Kan, M.S. Wong, C.Y.T. Kwok, X. Yu, Investigating the relationship between the built environment and relative risk of COVID-19 in Hong Kong, *ISPRS Int. J. Geo-Inf.* 9 (11) (2020), <https://doi.org/10.3390/ijgi9110624>.
- [25] Q.C. Nguyen, et al., Using 164 million google street view images to derive built environment predictors of COVID-19 cases, *Int. J. Environ. Res. Publ. Health* 17 (17) (2020) 1–13, <https://doi.org/10.3390/ijerph17176359>.
- [26] B. Wali, L.D. Frank, Neighborhood-level COVID-19 hospitalizations and mortality relationships with built environment, active and sedentary travel, *Health Place* 71 (2021), 102659, <https://doi.org/10.1016/j.healthplace.2021.102659>.
- [27] X. Li, L. Zhou, T. Jia, R. Peng, X. Fu, Y. Zou, Associating COVID-19 severity with urban factors: a case study of Wuhan, *Int. J. Environ. Res. Publ. Health* 17 (18) (2020) 1–20, <https://doi.org/10.3390/ijerph17186712>.
- [28] B. Li, Y. Peng, H. He, M. Wang, T. Feng, Built environment and early infection of COVID-19 in urban districts: a case study of Guangzhou, *Sustain. Cities Soc.* 66 (2021) 1–10, <https://doi.org/10.1016/j.scs.2020.102685>.
- [29] T.L. Yip, Y. Huang, C. Liang, Built environment and the metropolitan pandemic: analysis of the COVID-19 spread in Hong Kong, *Build. Environ.* 188 (2021), 107471, <https://doi.org/10.1016/j.buildenv.2020.107471>.
- [30] H. You, X. Wu, X. Guo, Distribution of covid-19 morbidity rate in association with social and economic factors in wuhan, China: implications for urban development, *Int. J. Environ. Res. Publ. Health* 17 (10) (2020), <https://doi.org/10.3390/ijerph17103417>.
- [31] Y. Han, et al., Spatial distribution characteristics of the COVID-19 pandemic in Beijing and its relationship with environmental factors, *Sci. Total Environ.* 761 (2019), 144257, <https://doi.org/10.1016/j.scitotenv.2020.144257>, 2021.
- [32] S. Li, S. Ma, J. Zhang, Association of built environment attributes with the spread of COVID-19 at its initial stage in China, *Sustain. Cities Soc.* 67 (2021), 102752, <https://doi.org/10.1016/j.scs.2021.102752>.
- [33] Z. Tianming, L. Helin, Exploration of the built-environmental elements that influence the spread of COVID-19 pandemic on community scale: a case study of wuhan, China, *Mod. Urban Res.* 10 (2020) 20–29, <https://doi.org/10.3969/j.issn.1009-6000.2020.10.003> (in Chinese).
- [34] Z. Kan, M.P. Kwan, M.S. Wong, J. Huang, D. Liu, Identifying the space-time patterns of COVID-19 risk and their associations with different built environment features in Hong Kong, *Sci. Total Environ.* 772 (2021), 145379, <https://doi.org/10.1016/j.scitotenv.2021.145379>.
- [35] H. Tong, M. Li, J. Kang, Relationships between building attributes and COVID-19 infection in London, *Build. Environ.* 225 (August) (2022), 109581, <https://doi.org/10.1016/j.buildenv.2022.109581>.
- [36] J.O. Klompmaker, et al., County-level exposures to greenness and associations with COVID-19 incidence and mortality in the United States, *Environ. Res.* 199 (2021), 111331, <https://doi.org/10.1016/j.envres.2021.111331>.
- [37] W. Lee, et al., Urban environments and COVID-19 in three Eastern states of the United States, *Sci. Total Environ.* 779 (2021), 146334, <https://doi.org/10.1016/j.scitotenv.2021.146334>.
- [38] B. Jiang, et al., Green spaces, especially nearby forest, may reduce the SARS-CoV-2 infection rate: a nationwide study in the United States, *Landsc. Urban Plann.* 228 (2022), 104583, <https://doi.org/10.1016/j.landurbplan.2022.104583>.
- [39] W. Peng, et al., City-level greenness exposure is associated with COVID-19 incidence in China, *Environ. Res.* 209 (2022), 112871, <https://doi.org/10.1016/j.envres.2022.112871>.
- [40] K.S. Lee, H.S. Min, J.H. Jeon, Y.J. Choi, J.H. Bang, H.K. Sung, The association between greenness exposure and COVID-19 incidence in South Korea: an ecological study, *Sci. Total Environ.* 832 (2022), 154981, <https://doi.org/10.1016/j.scitotenv.2022.154981>.
- [41] Y. You, S. Pan, Urban vegetation slows down the spread of coronavirus disease (COVID-19) in the United States, *Geophys. Res. Lett.* 47 (18) (2020) 1–9, <https://doi.org/10.1029/2020GL089286>.
- [42] C. Liu, Z. Liu, C.H. Guan, The impacts of the built environment on the incidence rate of COVID-19: a case study of King County, Washington, *Sustain. Cities Soc.* 74 (1239) (2021), 103144, <https://doi.org/10.1016/j.scs.2021.103144>.
- [43] T. Ciupa, R. Suligowski, Green-blue spaces and population density versus covid-19 cases and deaths in Poland, *Int. J. Environ. Res. Publ. Health* 18 (12) (2021), <https://doi.org/10.3390/ijerph18126636>.
- [44] K. Lata, K. Thapa, A.S. Rajput, Liveability of Indian cities and spread of covid-19 – case of tier-1 cities, *Indian J. Publ. Adm.* 67 (3) (2021) 365–382, <https://doi.org/10.1177/00195561211038063>.
- [45] Y. Zhang, N. Chen, W. Du, Y. Li, X. Zheng, Multi-source sensor based urban habitat and resident health sensing: a case study of Wuhan, China, *Build. Environ.* 198 (April) (2021), 107883, <https://doi.org/10.1016/j.buildenv.2021.107883>.
- [46] M. Coccia, Factors determining the diffusion of COVID-19 and suggested strategy to prevent future accelerated viral infectivity similar to COVID, *Sci. Total Environ.* 729 (2020), 138474, <https://doi.org/10.1016/j.scitotenv.2020.138474>.

- [47] A. Valsamatzis-Panagiotou, R. Penchovsky, Environmental factors influencing the transmission of the coronavirus 2019: a review, *Environ. Chem. Lett.* 20 (3) (2022) 1603–1610, <https://doi.org/10.1007/s10311-022-01418-9>.
- [48] M. Chen, F. Dai, B. Yang, S. Zhu, Effects of urban green space morphological pattern on variation of PM2.5 concentration in the neighborhoods of five Chinese megacities, *Build. Environ.* 158 (1–15) (2019), <https://doi.org/10.1016/j.buildenv.2019.04.058> [Online]. Available.
- [49] S. Wangxin, Z. Liukuan, C. Qing, Characteristics of blue-green infrastructure and its relationship with thermal environment in blocks based on morphological spatial pattern analysis (MSPA), *Chinese J. Ecol.* 41 (6) (2022) 1173–1181, <https://doi.org/10.13292/j.1000-4890.202205.015>.
- [50] T.F. Johnson, L.A. Hordley, M.P. Greenwell, L.C. Evans, Associations between COVID-19 transmission rates, park use, and landscape structure, *Sci. Total Environ.* 789 (2021), 148123, <https://doi.org/10.1016/j.scitotenv.2021.148123>.
- [51] J. Pan, R. Bardhan, Y. Jin, Spatial Divergent Effects of Public Green Space and COVID-19 Infection in London, vol. 62, *Urban For. Urban Green.*, 2021, 127182, <https://doi.org/10.1016/j.ufug.2021.127182>.
- [52] L. Wang, J. Zhao, Spatiotemporal distribution pattern of the COVID-19 epidemic and geographical detection, *Acta Ecol. Sin.* 40 (19) (2020) 6788–6800 (in Chinese).
- [53] S. Saura, P. Vogt, J. Velázquez, A. Hernando, R. Tejera, Key structural forest connectors can be identified by combining landscape spatial pattern and network analyses, *For. Ecol. Manage.* 262 (2) (2011) 150–160, <https://doi.org/10.1016/j.foreco.2011.03.017>.
- [54] P. Soille, P. Vogt, Morphological segmentation of binary patterns, *Pattern Recogn. Lett.* 30 (4) (2009) 456–459, <https://doi.org/10.1016/j.patrec.2008.10.015>.
- [55] S. Bi, F. Dai, M. Chen, S. Xu, A new framework for analysis of the morphological spatial patterns of urban green space to reduce PM2.5 pollution: a case study in Wuhan, China, *Sustain. Cities Soc.* 82 (2022), 103900, <https://doi.org/10.1016/j.scs.2022.103900>. March.
- [56] J. Lin, S. Qiu, X. Tan, Y. Zhuang, Measuring the relationship between morphological spatial pattern of green space and urban heat island using machine learning methods, *Build. Environ.* 228 (July 2022) (2023), 109910, <https://doi.org/10.1016/j.buildenv.2022.109910>.
- [57] J. Lin, C. Huang, Y. Wen, X. Liu, An assessment framework for improving protected areas based on morphological spatial pattern analysis and graph-based indicators, *Ecol. Indic.* 130 (2021), 108138, <https://doi.org/10.1016/j.ecolind.2021.108138>.
- [58] J. Rogan, et al., Forest fragmentation in Massachusetts, USA: a town-level assessment using Morphological spatial pattern analysis and affinity propagation, *GIScience Remote Sens.* 53 (4) (2016) 506–519, <https://doi.org/10.1080/15481603.2016.1141448>.
- [59] L. Wu, Z. Shengchuan, J. Xiaofeng, M. Jingwen, Impact of traffic exposure and land use patterns on the risk of COVID-19 spread at the community level, *China J. Highw. Transp.* 33 (11) (2020) 43–54, <https://doi.org/10.19721/j.cnki.1001-7372.2020.11.005> [Online]. Available.
- [60] Z. Liang, Y. Wang, F. Sun, C. Liang, S. Li, Geographical pattern of COVID-19 incidence of China's cities: role of migration and socioeconomic status, *Res. Environ. Sci.* 33 (7) (2020) 1571–1578, <https://doi.org/10.13198/j.issn.1001-6929.2020.05.45>.
- [61] M. Chen, J. Bai, S. Zhu, B. Yang, F. Dai, The influence of neighborhood-level urban morphology on PM2.5 variation based on random forest regression, *Atmos. Pollut. Res.* 12 (8) (2021), 101147, <https://doi.org/10.1016/j.apr.2021.101147>.
- [62] L. Breiman, Random forests, *Mach. Learn.* 45 (2001) 5–32, <https://doi.org/10.1023/A:1010933404324>.
- [63] Q. Wang, X. Wang, Y. Zhou, D. Liu, H. Wang, The dominant factors and influence of urban characteristics on land surface temperature using random forest algorithm, *Sustain. Cities Soc.* 79 (2022), 103722, <https://doi.org/10.1016/j.scs.2022.103722>.
- [64] Z. Wang, Z. Zhao, C. Wang, Random forest analysis of factors affecting urban carbon emissions in cities within the Yangtze River Economic Belt, *PLoS One* 16 (2021) 1–20, <https://doi.org/10.1371/journal.pone.0252337>.
- [65] J. Ai, et al., Epidemiologic characteristics and influencing factors of cluster infection of COVID-19 in Jiangsu Province, *Epidemiol. Infect.* 149 (e48) (2021) 1–8, <https://doi.org/10.1017/S0950268821000327>.
- [66] Y. Lu, et al., Green spaces mitigate racial disparity of health: a higher ratio of green spaces indicates a lower racial disparity in SARS-CoV-2 infection rates in the USA, *Environ. Int.* 152 (2021), <https://doi.org/10.1016/j.envint.2021.106465>.
- [67] F. Li, F. Li, S. Li, Y. Long, Science of the Total Environment Deciphering the recreational use of urban parks : experiments using multi-source big data for all Chinese cities, *Sci. Total Environ.* 701 (2020), 134896, <https://doi.org/10.1016/j.scitotenv.2019.134896>.
- [68] Y. Chen, Z. Luo, Hedonic pricing of houses in megacities pre- and post-COVID-19: a case study of Shanghai, China, *Sustainability* 14 (17) (2022), <https://doi.org/10.3390/su141711021>.
- [69] S. Bi, M. Chen, F. Dai, The impact of urban green space morphology on PM2.5 pollution in Wuhan, China: a novel multiscale spatiotemporal analytical framework, *Build. Environ.* 221 (2022), 109340, <https://doi.org/10.1016/j.buildenv.2022.109340>. June.
- [70] M. Lei, G. Jiang, J. Yang, X. Mei, P. Xia, L. Zhao, Thermal error modeling with dirty and small training sample for the motorized spindle of a precision boring machine, *Int. J. Adv. Manuf. Technol.* 93 (1–4) (2017) 571–586, <https://doi.org/10.1007/s00170-017-0531-7>.
- [71] J. Wu, X.Y. Chen, H. Zhang, L.D. Xiong, H. Lei, S.H. Deng, Hyperparameter optimization for machine learning models based on Bayesian optimization, *J. Electron. Sci. Technol.* 17 (1) (2019) 26–40, <https://doi.org/10.11989/JEST.1674-862X.80904120>.
- [72] M.M. Ramadhan, I.S. Sitanggang, F.R. Nasution, A. Ghifari, Parameter tuning in random forest based on Grid search method for gender classification based on voice frequency, *DEStech Trans. Comput. Sci. Eng., no. cece* (2017), <https://doi.org/10.12783/dtsc/cece2017/14611>.
- [73] S. Jiao, W. Chen, J. Wang, N. Du, Q. Li, G. Wei, Soil microbiomes with distinct assemblies through vertical soil profiles drive the cycling of multiple nutrients in reforested ecosystems, *Microbiome* 6 (1) (2018) 1–13, <https://doi.org/10.1186/s40168-018-0526-0>.
- [74] M.S. Alam, R. Sultana, Influences of climatic and non-climatic factors on COVID-19 outbreak: a review of existing literature, *Environ. Challenges* 5 (2021), 100255, <https://doi.org/10.1016/j.envc.2021.100255>.
- [75] E.L. Anderson, P. Turnham, J.R. Griffin, C.C. Clarke, Consideration of the aerosol transmission for COVID-19 and public health, *Risk Anal.* 40 (5) (2020) 902–907, <https://doi.org/10.1111/risa.13500>.
- [76] N. Wilson, S. Corbett, E. Tovey, Airborne transmission of covid-19, *BMJ* 370 (2020) 10–11, <https://doi.org/10.1136/bmj.m3206>.
- [77] Y. Zhu, J. Xie, F. Huang, L. Cao, Association between short-term exposure to air pollution and COVID-19 infection: evidence from China, *Sci. Total Environ.* 727 (2020), 138704, <https://doi.org/10.1016/j.scitotenv.2020.138704>.
- [78] M.F. Bashir, et al., Correlation between environmental pollution indicators and COVID-19 pandemic: a brief study in Californian context, *Environ. Res.* 187 (2020), 109652, <https://doi.org/10.1016/j.envres.2020.109652>.
- [79] J. Xie, Y. Zhu, Association between ambient temperature and COVID-19 infection in 122 cities from China, *Sci. Total Environ.* 724 (2020), 138201, <https://doi.org/10.1016/j.scitotenv.2020.138201>.
- [80] R. Tosepu, et al., Correlation between weather and covid-19 pandemic in jakarta, Indonesia, *Sci. Total Environ.* 725 (2020), <https://doi.org/10.1016/j.scitotenv.2020.138436>.
- [81] M. Jerrett, et al., Air pollution and meteorology as risk factors for COVID-19 death in a cohort from Southern California, *Environ. Int.* 171 (December 2022) (2023), 107675, <https://doi.org/10.1016/j.envint.2022.107675>.
- [82] L. Martelletti, P. Martelletti, Air pollution and the novel covid-19 disease: a putative disease risk factor, *SN Compr. Clin. Med.* 2 (4) (2020) 383–387, <https://doi.org/10.1007/s42399-020-00274-4>.
- [83] H. Li, X.L. Xu, D.W. Dai, Z.Y. Huang, Z. Ma, Y.J. Guan, Air pollution and temperature are associated with increased COVID-19 incidence: a time series study, *Int. J. Infect. Dis.* 97 (2020) 278–282, <https://doi.org/10.1016/j.ijid.2020.05.076>.
- [84] W. Kuang, Seasonal variation in air temperature and relative humidity on building areas and in green spaces in Beijing, China, *Chin. Geogr. Sci.* 30 (1) (2020) 75–88, <https://doi.org/10.1007/s11769-020-1097-0>.
- [85] X.D. Xiao, L. Dong, H. Yan, N. Yang, Y. Xiong, The influence of the spatial characteristics of urban green space on the urban heat island effect in Suzhou Industrial Park, *Sustain. Cities Soc.* 40 (April) (2018) 428–439, <https://doi.org/10.1016/j.scs.2018.04.002>.
- [86] D.P.M. Junior, C. Bueno, C.M. da Silva, The effect of urban green spaces on reduction of particulate matter concentration, *Bull. Environ. Contam. Toxicol.* 108 (6) (2022) 1104–1110, <https://doi.org/10.1007/s00128-022-03460-3>.
- [87] H.A. Aboubakar, T.A. Sharafeldin, S.M. Goyal, Stability of SARS-CoV-2 and other coronaviruses in the environment and on common touch surfaces and the influence of climatic conditions: a review, *Transbound. Emerg. Dis.* 68 (2) (2021) 296–312, <https://doi.org/10.1111/tbed.13707>.